Materials Horizons

ROYAL SOCIETY OF CHEMISTRY

OPINION

View Article Online
View Journal | View Issue

Cite this: *Mater. Horiz.*, 2025, **12**, 1381

Rational design of uniform SiO_2-based afterglow microparticles for photonic crystals

Gaoqiang Li,† Mengfen Che,† Xue Chen and Xiaowang Liu *

Despite recent advancements in organic phosphors, the synthesis of monodisperse afterglow microparticles (MPs) suitable for creating photonic crystals remains challenging. The SiO_2 matrix is an attractive host material for activating the long-lived emissions of doped molecules due to several factors, including its cross-linked polymer-like structure, abundance of –OH groups, robustness, and presence of numerous emitter defects. However, the Stöber method struggles to produce monodisperse molecule-doped SiO_2 MPs due to the complexity of the system. Our reported pseudomorphic transformation-assisted doping method shows promise in addressing this issue by using monodisperse SiO_2 MPs as parent materials in the presence of dopants under hydrothermal conditions. This method offers flexibility in controlling the optical properties of the resulting monodisperse molecule-doped SiO_2 MPs. The uniformity allows for the assembly of afterglow SiO_2 MPs into photonic crystals, which demonstrate not only afterglow but also angle-dependent structural colors. Furthermore, adjusting the match between the stopband of the photonic crystals and the emission bands of the doped molecules presents additional opportunities to tune the optical properties of the assemblies. Our findings significantly expand the applications of afterglow materials in fields such as information storage and anticounterfeiting.

Received 30th October 2024,
Accepted 13th December 2024

DOI: 10.1039/d4mh01541j

rsc.li/materials-horizons

Need for the synthesis of uniform and robust organic afterglow microparticles (MPs)

Room-temperature organic afterglow materials represent an emerging class of luminescent materials characterized by their large Stokes shifts, high signal-to-noise ratios, and long luminescence lifetimes.[1–3] In contrast to inorganic phosphors, organic alternatives offer superior processability and are well-suited for the fabrication of large-area, transparent films, making them highly compatible with organic electronics.[4–6] Significant progress has been made in designing organic afterglow materials through various approaches, including crystallization engineering,[7] H-aggregation,[8] dopant stabilization in rigid matrices,[9] and polymerization.[10] Strong dopant–matrix interactions—such as covalent bonding, hydrogen bonding, and physical fixation—play a critical role in stabilizing *in situ*-generated triplet states and minimizing non-radiative relaxation, enabling bright afterglow from the dopants.[11] Furthermore, triplet-to-singlet energy transfer provides tunable afterglow emission across the visible spectrum, depending on the selection of energy donor–acceptor pairs.[12–15]

Currently, organic afterglow materials are primarily available in bulk forms, such as polymer films and crystals, largely limiting their applications.[16,17] In addition, their afterglow properties are often susceptible to solvents due to the swelling behavior of polymer matrices and the instability of crystals in solvent environments.[18] The synthesis of uniform and monodisperse micro-sized organic afterglow particles remains a formidable challenge. Achieving this synthesis would be highly advantageous, as it would enable the straightforward creation of photonic crystals—periodic dielectric structures that are designed to form the energy band structure for photons.[19] This optical platform can further manipulate afterglow properties by modulating the optical density of states, in addition to producing other unique optical phenomena, such as angle-dependent structural colors.[20–22]

SiO_2 as a versatile host matrix

Drawing inspiration from established principles in the synthesis of organic afterglow materials, we identified suitable combinations of microsized hosts and dopants as a vital solution. The SiO_2 matrix exhibits several key characteristics that make it a versatile host material for the synthesis of

Frontiers Science Center for Flexible Electronics (FSCFE), MIIT Key Laboratory of Flexible Electronics (KLoFE), Shaanxi Key Laboratory of Flexible Electronics, Xi'an Key Laboratory of Flexible Electronics, Xi'an Key Laboratory of Biomedical Materials & Engineering, Xi'an Institute of Flexible Electronics, Institute of Flexible Electronics (IFE), Northwestern Polytechnical University, Xi'an 710072, Shaanxi, China. E-mail: iamxwliu@nwpu.edu.cn

† These two authors contributed equally to this work.

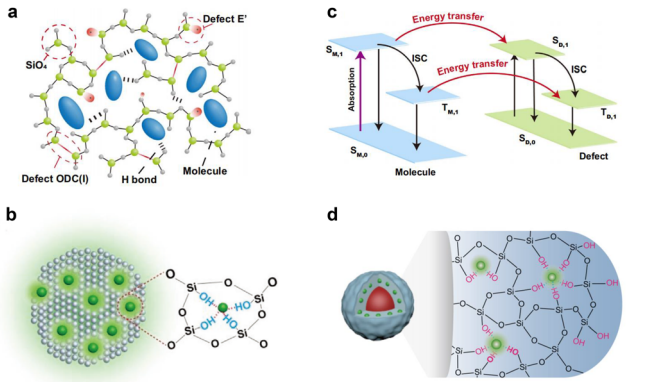

Fig. 1 The attractiveness of SiO_2 matrix as host materials for the synthesis of organic afterglow phosphors. (a) Schematic depiction of SiO_2 matrix structure suitable for molecule doping.[21] Copyright 2024, Springer Nature. (b) Afterglow activation mechanism.[20] Copyright 2023, Wiley-VCH. (c) Schematic illustration of energy transfer between molecule dopants and SiO_2 defects for afterglow tuning.[21] Copyright 2024, Springer Nature. (d) Schematic illustration of the construction of multifunction SiO2-based MPs through the shell@shell structure.

organic afterglow phosphors: (i) the SiO_2 matrix features a cross-linked polymer-like structure, with SiO_4 units interconnected by Si–O groups (Fig. 1a). This configuration allows doped organic emitters to be effectively trapped by the polymer-like chains, stabilizing the *in situ* generated triplet states.[23] (ii) The abundance of –OH groups within the SiO_2 matrix plays a crucial role. Imperfect SiO_4 units create numerous –OH groups, which interact more strongly with doped organic emitters through hydrogen bonding and, at elevated temperatures, even covalent bonding. Imperfect SiO_4 units also result in a loose internal microstructure, facilitating the incorporation of organic dopants and enhancing doping efficiency.[24] (iii) The robustness of the SiO_2 matrix prevents swelling in various solvents, ensuring effective separation of organic dopants from quenchers (Fig. 1b). This characteristic contributes to the excellent stability of the organic afterglow. (iv) The presence of numerous emitter defects within the SiO_2 matrix, such as E′-defects, H-defects, and PRHT defects, allows for tailored energy transfer with doped organic emitters, enabling rational tuning of the optical properties of the resultant organic-emitter-doped SiO_2 materials (Fig. 1c).[25–27] (v) The well-established Stöber method enables the uniform synthesis of SiO_2 microspheres with a single-size distribution, paving the possibility for the production of monodisperse emitter-doped SiO_2 through careful adjustment of experimental conditions.[28] (vi) In SiO_2, the electron-deficient silicon sites allow the formation of coordination bonds with ligands containing atoms with a lone pair of electrons, enabling additional stabilization of the triplet states of the molecule dopants upon excitation.[29]

In addition, SiO_2 exhibits a refractive index of 1.46, which creates a significant contrast with air and contributes to the formation of a sharp, strong reflection band in photonic crystals. The inherent stability of SiO_2 further ensures the consistent performance of these crystals across diverse environmental conditions. Moreover, the chemical stability of SiO_2 MPs preserves both their structure and optical properties over extended periods. The SiO_2 matrix is also recognized as an effective coating material, facilitating the growth of various nano- and micro-sized particles, enhancing biocompatibility, and enabling easier surface modifications. Recent advances in SiO_2 coating and doping strategies have enabled the development of multifunctional afterglow composites (Fig. 1d), greatly enriching the optical properties of core-only materials.[30]

Pseudomorphic transformation-assisted doping as a potential game changer

While the Stöber method is attractive for *in situ* doping of emitters to create afterglow materials, achieving a uniform single-size distribution of SiO_2-based MPs as building blocks remains a significant challenge. Several issues arise: (i) organic dopants often exhibit limited solubility in the typical water-ethanol solvent mixture used in the Stöber method, complicating synthesis control and limiting the exploration of potential dopant libraries. (ii) The introduction of organic dopants can disrupt the hydrolysis kinetics of the SiO_2 precursor tetraethoxysilane (TEOS), leading to poor control over the morphology of the doped SiO_2 particles. Moreover, nanosized dopants, such as carbon dots (CDs), may result in afterglow nanocomposites that are unsuitable for photonic crystal fabrication. (iii) Finally, organic molecule-doped SiO_2 materials synthesized *via* the Stöber method often exhibit a loose internal microstructure, raising concerns about the leakage of dopants and diffusion of solvent molecules, which can compromise the stability of afterglow emission in the resultant doped SiO_2 phosphors.[31]

Our recently developed pseudomorphic transformation-assisted doping addresses the aforementioned concerns effectively (Fig. 2). This strategy employs hydrothermal treatment of a mixture of organic dopants and single-sized SiO_2 MPs in an aqueous solution at elevated temperatures. The single-sized SiO_2 MPs, pre-synthesized *via* the Stöber method, undergo three key stages. In the first stage, increasing the reaction temperature leads to the dissolution of the surface layer of the parent SiO_2 MPs, forming orthosilicic acid and enhancing the concentration of dissolved organic dopants. This stage culminates in equilibrium between the dissolution of SiO_2 and the recondensation of orthosilicic acid on the etched SiO_2 MPs. In the second stage, defects on the etched SiO_2 MPs interact with the organic dopants, trapping them as the newly formed SiO_2 matrix coats the dopants, resulting in the formation of organic emitter-doped SiO_2 MPs. This iterative process produces restructured emitter-doped SiO_2 MPs. In the third stage, additional SiO_2 matrix growth occurs on the surfaces of the previously formed MPs upon cooling, leading to the final products. Our results demonstrate that our strategy is applicable to various nanosized dopants, including CDs and molecular dopants such as 4-phenylpyridine (4-PP), 4,4′-bipyridine (4,4-BP), and 1,4-bis(pyrid-4-yl)benzene (1,4-DPB), leading

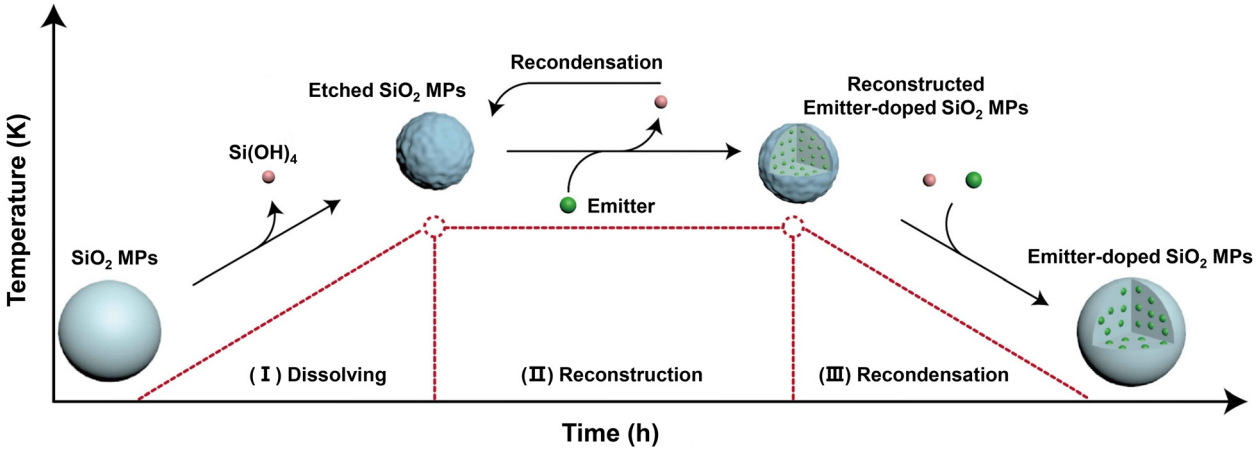

Fig. 2 Schematic representation of pseudomorphic transformation-assisted doping for the synthesis of monodisperse afterglow SiO_2 MPs. The strategy mainly involves three steps: (i) dissolution of the surface layer of SiO_2 MPs under hydrothermal conditions with the formation of orthosilicic acid at elevated temperatures; (ii) doping of emitter molecules (nanoparticles) into the SiO_2 matrix through an equilibrium of hydrolysis and repolymerization of the SiO_2 framework; and (iii) recondensation of the dissolved orthosilicic acid when cooling the reaction further encapsulating the emitter with the formation of monodisperse afterglow emitter-doped SiO_2 MPs.[21]

to the formation of doped SiO_2 MPs with a uniform size distribution (Fig. 3a). For nanosized dopants, the afterglow properties of the resultant CD-doped SiO_2 MPs—such as afterglow wavelength, lifetime, and quantum yields—are primarily influenced by the characteristics of the CDs.[32–34] Strong interactions between the SiO_2 matrix and the CDs can further enhance the afterglow attributes. It is important to note that the nanosized dopants must have a diameter of less than 6 nm;

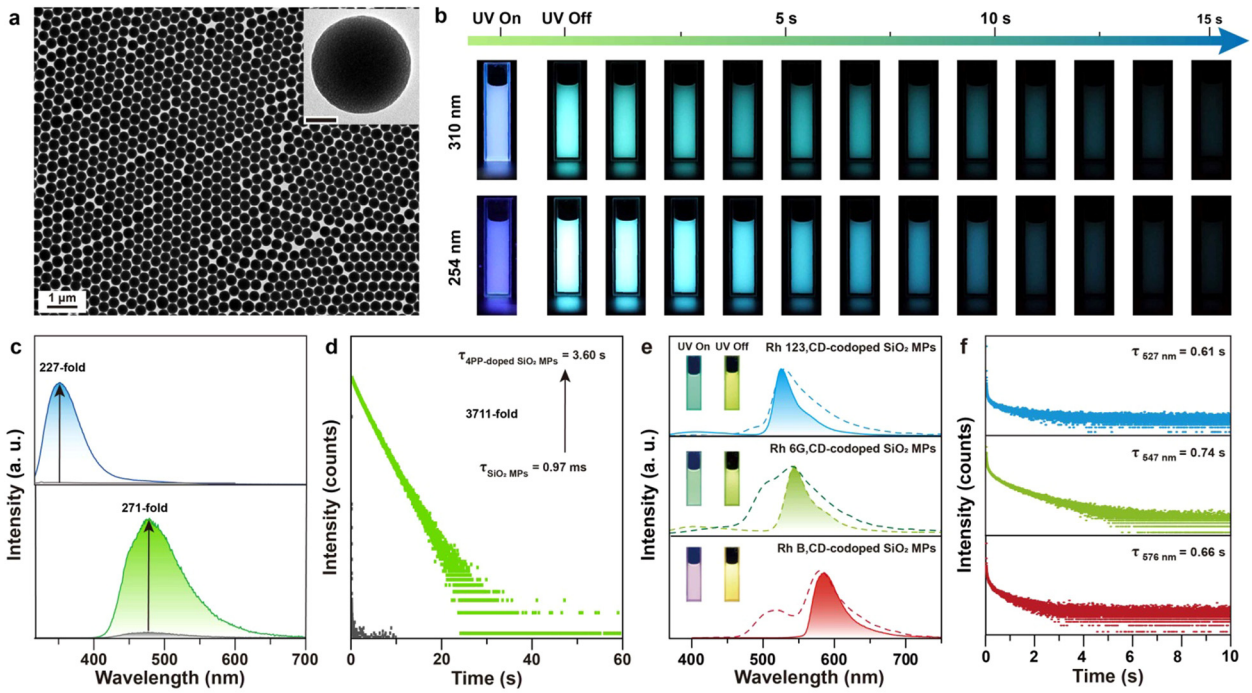

Fig. 3 Characterization of SiO_2-based afterglow MPs. (a) TEM image of 4-PP-doped SiO_2 MPs. Inset: High-magnification TEM image displaying a single 4-PP-doped SiO_2 MP. Scale bar: 100 nm. (b) Luminescence photographs depicting an aqueous dispersion of 4-PP-doped SiO_2 MPs. (c) Comparative short- and long-lived emission of corresponding aqueous dispersions of 4-PP-doped SiO_2 MPs and SiO_2 MPs (10 mg mL^{-1}). (d) Decay curves at 472 nm for SiO_2 MPs and 4-PP-doped SiO_2 MPs. (a)–(d) Reproduced with permission.[21] Copyright 2024, Springer Nature. (e) The photoluminescence spectra of CD, dye-codoped SiO_2 MPs. The dash lines show the fluorescence profiles, while the solid lines display the delay profiles (delay time: 2 ms). Inset: Luminescence photographs of the corresponding aqueous dispersions of CD,dye-codoped SiO_2 MPs. (f) Decay curves of the triplet-sensitized-fluorescence of the corresponding dyes. Note that the codoped dyes are Rh 123, Rh 6G and Rh B from top to bottom, respectively. (e) and (f) Reproduced with permission.[20] Copyright 2023, Wiley-VCH.

exceeding this critical size weakens the trapping of nanoparticles (NPs) by defects on the surface of the etched SiO_2 MPs, leading to the formation of NP aggregate@SiO_2 impurities in the products. In contrast, molecular dopants offer distinct advantages (Fig. 3b–d): the wide variety available facilitates the generation of afterglow across the entire visible spectrum and simplifies the separation of undoped dopants from the resultant molecule-doped SiO_2 MPs. Additionally, at temperatures above 150 °C, organic dopants show increased solubility and strong defect-molecule interactions, enhancing their effective incorporation into the SiO_2 matrix.

Our strategy demonstrates a strong capability for tuning the afterglow properties of the resultant emitter-doped SiO_2 MPs. A commonly used method involves codoping multiple emitters into SiO_2 MPs through a single-pot hydrothermal reaction. Different dopants exhibit distinct responses to excitation at specific wavelengths, enabling the creation of excitation-dependent afterglow SiO_2 MPs. However, a challenge with this method is that various organic dopants display differing solubility in water and interact differently with the SiO_2 matrix, complicating precise control over the doping levels of each emitter. An alternative approach involves co-doping dye molecules, which predominantly exhibit singlet emissions, with afterglow emitters to modulate the afterglow characteristics. In this method, the tuning of afterglow in the codoped system relies on energy transfer from triplet dopants to singlet dyes. Our results show a decrease in the lifetime of the CD afterglow, accompanied by the emergence of long-lived dye emissions, suggesting a Förster resonance energy transfer (FRET) mechanism. This approach is particularly advantageous for

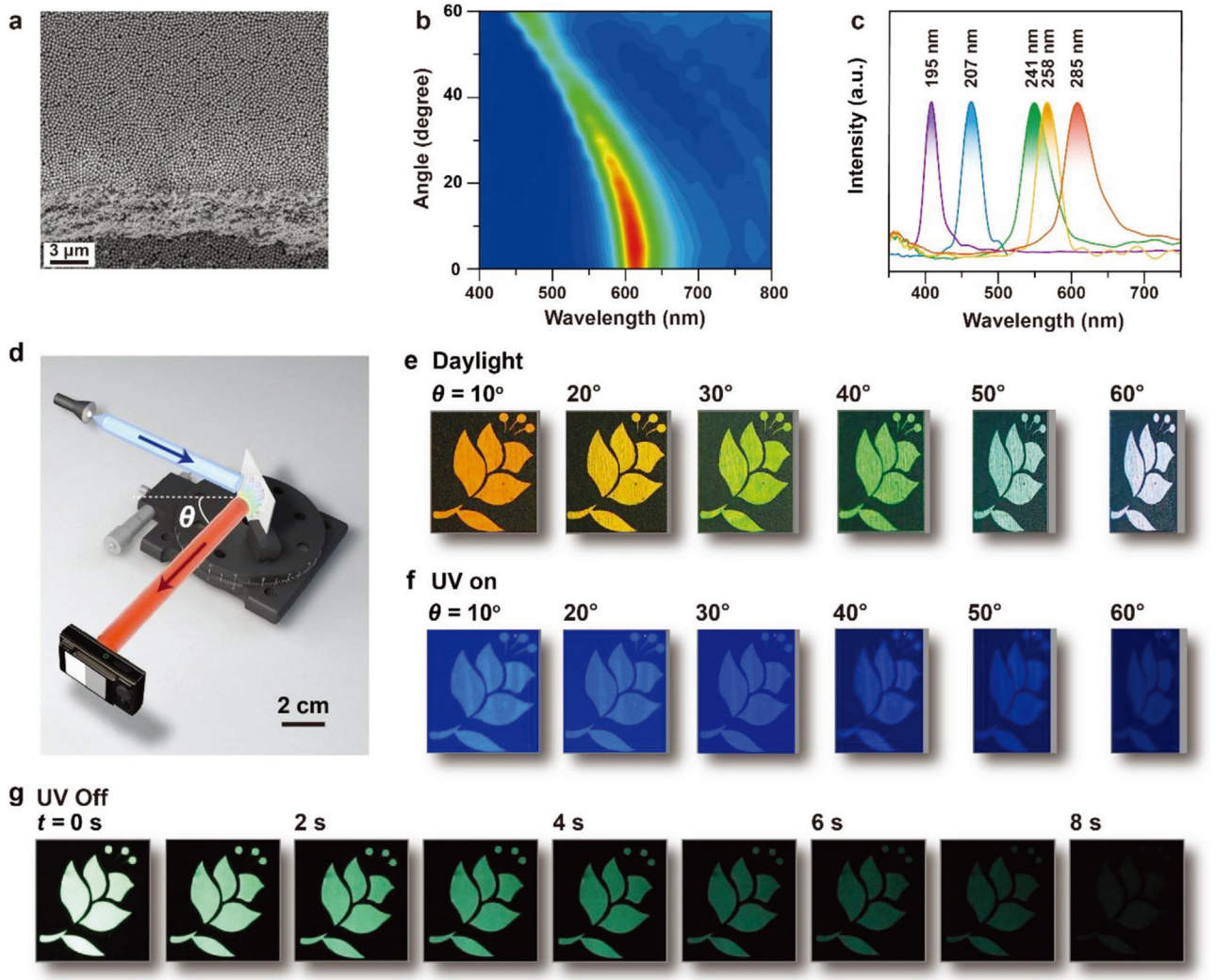

Fig. 4 Characterization and application of photonic crystals prepared by CD-doped afterglow MPs. (a) Scanning electron microscopy image of a photonic crystal comprising CD-doped SiO_2 MPs. (b) Color-filled contour maps of the normalized reflectance spectra. (c) Reflection spectra of PCs that are formed by CD-doped SiO_2 MPs with different diameters at an angle of 10°. (d) A custom-made stage designed for studying the angle-dependent structural colors and luminescence presentation of PCs. (e) The angle-dependent structural colors of the as-prepared flower-shaped photonic crystal under daylight. (f) Angle-dependent luminescence images of the pattern upon UV excitation. (g) Time-dependent afterglow images of the pattern after ceasing excitation taken at an observation angle of 10°. (a)–(g) Reproduced with permission.[20] Copyright 2023, Wiley-VCH.

generating afterglow emissions in the red or near-infrared spectral regions. Additionally, FRET can be designed to occur from doped CDs to transition metal ions, such as Mn^{2+}, to achieve red afterglow emissions.[35] Recently, we reported utilizing energy interactions between dopants and intrinsic SiO_2 defects to adjust the afterglow emissions of doped SiO_2 MPs. This method offers the benefit of rationally controlling the lowest triplet energy levels through the careful selection of suitable dopants, thereby facilitating energy transfer from the dopants to various emissive defects in the SiO_2 matrix (Fig. 3e and f). Despite observing excitation-dependent afterglow resulting from energy transfer to defects, identifying the specifics of the emissive defects remains a challenging task.

An additional benefit of our strategy is the remarkable robustness of the afterglow exhibited by emitter-doped SiO_2 MPs. The long afterglow of CD-doped SiO_2 MPs remains visible to the naked eye in aqueous solutions, even in the presence of transition metal ions such as Fe^{3+}, Ni^{2+}, and Ce^{3+}. Removing these transition metal ions allows for complete recovery of the afterglow luminescence, due to effective separation of the dopants from the quenchers. Furthermore, the uniformity of the single-sized SiO_2 MPs ensures consistent participation in subsequent reactions, facilitating the large-scale synthesis of afterglow SiO_2 MPs with a uniform size distribution. Our lab has successfully demonstrated kilogram-scale synthesis. It is important to note that as we scale up the synthesis, the reaction time needs to be extended accordingly, typically requiring double the reaction time to achieve the same afterglow properties. This is understandable, as the reaction system requires more time to reach dissolution-redeposition equilibrium at larger scales. In addition, the size of the resultant afterglow emitter-doped SiO_2 MPs is slightly smaller than that of the original parent SiO_2 MPs due to the presence of a slight excess of SiO_2 precursor in the reaction mixture. We further estimate the cost of producing afterglow SiO_2 MPs to be approximately \$0.30 per gram, highlighting their great potential for practical applications. The main cost contributors are the TEOS and solvent used in the synthesis. The cost of the doped molecules is negligible, as the doping concentration is typically less than 0.15 wt%.

The successful large-scale synthesis of SiO_2-based afterglow MPs with a uniform size distribution facilitates the straightforward creation of photonic crystals (Fig. 4a). Our results demonstrate that the dip-coating method enables the assembly of these afterglow SiO_2 MPs into highly ordered structures. Additionally, the resulting afterglow SiO_2 MP films exhibit angle-dependent refraction, a characteristic feature of photonic crystals (Fig. 4b). The refraction spectrum can be further tuned by using different sizes of afterglow SiO_2 MPs as building blocks for photonic crystal fabrication (Fig. 4c). Moreover, SiO_2 photonic crystal films can be patterned into well-defined designs using laser beams. For instance, a rose-shaped pattern was fabricated and displayed a color shift from orange to blue as the incident angle increased (Fig. 4d and e). Simultaneously, the fluorescence intensity weakened, likely due to reduced excitation efficiency at higher incident angles (Fig. 4f).

The structural color transition with changing observation angles can be explained by the following equation:[36]

$$\lambda_{max} = 1.633(d/m)(n_a{}^2 - \sin^2\theta)^{1/2}$$

where d is the diameter of the MPs, m represents the Bragg reflection order, and θ is the angle between the incident light and the normal to the surface. The effective refractive index, n_a, is defined as the weighted sum of the refractive indices of the MPs and the voids between them. In addition, the pattern displays a strong green afterglow that can last for over 8 seconds (Fig. 4g).

The ease of growing afterglow SiO_2 layers on MPs with high refractive indices demonstrates the potential to enhance the scattering efficiency of photonic crystals. One example involves the use of ZnS@CD-doped SiO_2 MPs as building blocks to fabricate photonic crystals. Note that the growth of a thin CD-doped SiO_2 layer not only imparts afterglow attributes but also improves the colloidal stability of ZnS MPs, enabling enhanced uniformity of the resultant photonic crystals.

New opportunity—additional optical tuning

Pseudomorphic transformation-assisted doping facilitates the synthesis of monodisperse SiO_2 MPs with carefully designed size distributions and optical properties. This capability significantly enhances the flexibility in tuning the optical characteristics of highly ordered SiO_2 MP assemblies, particularly in photonic crystal applications. It is well established that the optical density of states within the photonic bandgap is limited. By meticulously aligning the fluorescence and phosphorescence bands with the stopband, we can effectively modulate the long-lived emission properties of these assemblies.

To improve the efficiency of long-lived emissions, accelerating the intersystem crossing process is crucial, as this reduces the proportion of short-lived emissions. As shown in Fig. 5, aligning the stopband with the fluorescence band can lead to several phenomena. First, the fluorescence from the organic emitters may diminish due to the reduced photonic density of states. Furthermore, the efficiency of intersystem crossing can be enhanced as the fluorescence process is suppressed. Notably, photonic bands have minimal impact on phosphorescence, thereby preserving the long-lived emission characteristics.[37] This contrasts with the heavy-atom effect observed in organic phosphorescence, which can improve efficiency but often shortens the emission lifetime due to an accelerated spin–flip process during the deactivation of triplet states.

Additionally, shifting the photonic band to coincide with the phosphorescence band of the doped organic emitters can extend the lifetime of their long-lived emissions by lowering the optical density of states. The matched photonic bands may even induce splitting of the long-lived emission bands, offering a precise means to fine-tune the optical properties of the afterglow. Alternatively, surface modification of uniform afterglow SiO_2 MPs with optically active molecules provides

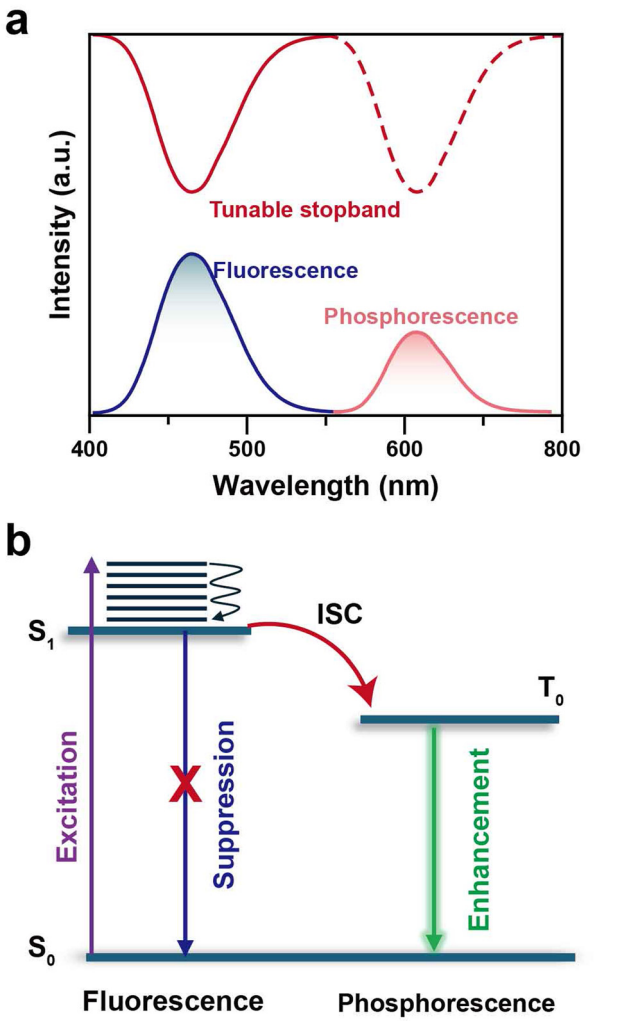

Fig. 5 Tuning optical properties in photonic crystal assemblies through the alignment of stopband characteristics with the photoluminescence of doped emitters. (a) Modulating the matching degree between the stopband and afterglow band to regulate emission intensity and lifetime. (b) Adjusting the alignment between the stopband and fluorescence band to reduce fluorescence, thus enhancing afterglow emission.

additional opportunities for tuning the resulting afterglow. For example, the covalent attachment of spiropyran molecules to SiO_2 MPs enables modulation of the optical properties by controlling the excitation durations.[38]

Concluding remarks

Pseudomorphic transformation-assisted doping provides an effective method for producing monodisperse SiO_2-based afterglow MPs, creating a new class of building blocks for photonic crystal development. For fundamental studies, establishing a comprehensive library of molecules with corresponding afterglow properties is essential, as it will guide the synthesis of SiO_2-based afterglow MPs. Currently, the organic dopants utilized typically contain nitrogen atoms, which facilitate excitation absorption through n → π* transitions and enhance spin–orbit coupling, ultimately increasing the population of the triplet state *via* an efficient intersystem crossing. However, the detailed interactions between these molecules and the SiO_2 matrix remain largely unexplored and require further investigation.

In photonic crystal applications, an important direction is extending these structures from solid to liquid states. The uniform size distribution of SiO_2-based MPs allows for precise control over their interactions during precipitation, leading to the formation of uniform SiO_2 MP clusters in solution. This homogeneous distribution gives rise to liquid photonic crystals, which exhibit angle-dependent structural colors in addition to their afterglow properties. These liquid photonic crystals enable direct tuning of optical properties by adjusting the alignment of the stopband with the emission bands of the doped organic emitters.

Moreover, the developed afterglow photonic crystals open up diverse applications. The combination of afterglow emissions and angle-dependent structural colors significantly enhances their potential in anti-counterfeiting and information coding. Additionally, these photonic crystals can serve as analytical platforms that present binary responses to analytes, improving selectivity and sensitivity. Consequently, our strategy for the rational synthesis of uniform SiO_2-based afterglow MPs greatly extends the methodology for developing optical materials and enhances the practical utility of these MPs, transforming afterglow SiO_2 MPs from a conceptual stage to real-world applications.

Data availability

As this is an opinion paper, the data supporting the arguments presented in this study can be found in the cited references.

Conflicts of interest

There are no conflicts to declare.

Acknowledgements

This work is supported by the National Natural Science Foundation of China (grant number 22075228), and the Fundamental Research Funds for the Central Universities (grant numbers 0515022GH0202036 and 23GH0202078).

Notes and references

1 S. Xu, R. Chen, C. Zheng and W. Huang, *Adv. Mater.*, 2016, **28**, 9920.
2 Y. Zhang, L. Chen, B. Liu, S. Yu, Y. Yang and X. Liu, *Adv. Funct. Mater.*, 2024, **34**, 2315366.
3 X. Wei, J. Yang, L. Hu, Y. Cao, J. Lai, F. Cao, J. Gu and X. Cao, *J. Mater. Chem. C*, 2021, **9**, 4425–4443.
4 X. Zheng, Q. Han, Q. Lin, C. Li, J. Jiang, Q. Guo, X. Ye, W. Z. Yuan, Y. Liu and X. Tao, *Mater. Horiz.*, 2023, **10**, 197–208.

5 G. Yin, W. Lu, J. Huang, R. Li, D. Liu, L. Li, R. Zhou, G. Huo and T. Chen, *Aggregate*, 2023, **4**, e344.
6 S. Sun, Y. Zhu, T. Li, G. Wang, F. Yin, F. Li, F. Tao, L. Wang and G. Li, *Chem. Eng. J.*, 2024, **485**, 149751.
7 S. S. Behera, A. Ghorai, S. Garain, R. V. Nair, S. J. George and K. S. Narayan, *Adv. Opt. Mater.*, 2023, **11**, 2300931.
8 W. Luo, J. Zhou, Y. Nie, F. Li, S. Cai, G. Yin, T. Chen and Z. Cai, *Adv. Funct. Mater.*, 2024, **34**, 2401728.
9 K. Chen, Y. Zhang, Y. Lei, W. Dai, M. Liu, Z. Cai, H. Wu, X. Huang and X. Ma, *Nat. Commun.*, 2024, **15**, 1269.
10 X. Dou, X. Wang, X. Xie, J. Zhang, Y. Li and B. Tang, *Adv. Funct. Mater.*, 2024, **34**, 2314069.
11 C. Zhang, F. Sun and Y. He, *ACS Appl. Mater. Interfaces*, 2023, **15**, 9970–9977.
12 S. Surendran Rajasree, J. Yu, H. C. Fry, R. Anderson, W. Xu, R. Krishnan, J. Duan, S. Goswami, D. A. Gómez-Gualdrón and P. Deria, *Angew. Chem., Int. Ed.*, 2023, **62**, e202305323.
13 X. Yang, G. I. N. Waterhouse, S. Lu and J. Yu, *Chem. Soc. Rev.*, 2023, **52**, 8005.
14 N. Xue, H.-Y. Zhou, Y. Han, M. Li, H.-Y. Lu and C.-F. Chen, *Nat. Commun.*, 2024, **15**, 1425.
15 S. Guan, X. Chen, R. Yu, W. Xu, Z. Wu, Y. D. Suh, X. Liu and W. Huang, *Angew. Chem., Int. Ed.*, 2024, e202415632.
16 Y. Miao, F. Lin, D. Guo, J. Chen, K. Zhang, T. Wu, H. Huang, Z. Chi and Z. Yang, *Sci. Adv.*, 2024, **10**, eadk3354.
17 R. Tian, S. Gao, K. Li and C. Lu, *Nat. Commun.*, 2023, **14**, 2720.
18 J. Huang, X. Deng, J. Li, G. Wang, X. Li, H. Yao, C. Lei and K. Zhang, *Chem. Eng. J.*, 2023, **474**, 145809.
19 H. Huang, J. Yin, Q. Zhou, H. Li, J. Yang, Y. Wang, M. Xu and C. Wang, *Nat. Commun.*, 2024, **15**, 3999.
20 X. Chen, Y. Wang, C. Peng, W. Hu, Z. Wu, W. Xu, S. Wu, Z. Luo, Y. D. Suh, T. S. Atabaev, X. Li, X. Liu and W. Huang, *Adv. Mater.*, 2023, **35**, 2307198.
21 X. Chen, M. Che, W. Xu, Z. Wu, Y. D. Suh, S. Wu, X. Liu and W. Huang, *Nat. Commun.*, 2024, **15**, 8111.
22 X. Q. Yu, J. Wu, J. W. Wang, N. X. Zhang, R. K. Qing, G. X. Li, Q. Li and S. Chen, *Adv. Mater.*, 2024, **36**, 2312879.
23 Y. Sun, S. Liu, L. Sun, S. Wu, G. Hu, X. Pang, A. T. Smith, C. Hu, S. Zeng, W. Wang, Y. Liu and M. Zheng, *Nat. Commun.*, 2020, **11**, 5591.
24 Y.-C. Liang, Q. Cao, K.-K. Liu, X.-Y. Peng, L.-Z. Sui, S.-P. Wang, S.-Y. Song, X.-Y. Wu, W.-B. Zhao, Y. Deng, Q. Lou, L. Dong and C.-X. Shan, *ACS Nano*, 2021, **15**, 16242.
25 J. He, Y. Chen, Y. He, X. Xu, B. Lei, H. Zhang, J. Zhuang, C. Hu and Y. Liu, *Small*, 2020, **16**, 2005228.
26 W. H. Green, K. P. Le, J. Grey, T. T. Au and M. J. Sailor, *Science*, 1997, **276**, 1826.
27 H. Chang, Y. Park, K. Kim, C. Han, Y. Yoon, W. Yoo, J. Yoo, D. Lee, H. Han, K. Kim, J. Joo and W. Kwon, *Chem. Eng. J.*, 2024, **493**, 152529.
28 S. Luo, Y. Li, W. Yang, W. Gao, H. Yu and N. Huang, *ACS Appl. Mater. Interfaces*, 2023, **15**, 33848.
29 A. Rimola, D. Costa, M. Sodupe, J.-F. Lambert and P. Ugliengo, *Chem. Rev.*, 2013, **113**, 4216–4313.
30 Z. Hossein, T. Du, L. Zhao, S. Zhu, Z. Su, K. Wang, B. Cui, Z. Tan, G. Fan and Z. Li, *Carbon*, 2024, **229**, 119449.
31 W. Zhang, Y. Liu, H. S. Jeppesen and N. Pinna, *Nat. Commun.*, 2024, **15**, 5463.
32 Y. Liu, M. Al-salihi, Y. Guo, R. Ziniuk, S. Cai, L. Wang, Y. Li, Z. Yang, D. Peng, K. Xi, Z. An, X. Jia, L. Liu, W. Yan and J. Qu, *Light: Sci. Appl.*, 2022, **11**, 163.
33 W. Li, S. Wu, X. Xu, J. Zhuang, H. Zhang, X. Zhang, C. Hu, B. Lei, C. F. Kaminski and Y. Liu, *Chem. Mater.*, 2019, **31**, 9887.
34 J. Chen, J. Tan, P. Liang, C. Wu, Z. Hou, K. Shen, B. Lei, C. Hu, X. Zhang, J. Zhuang, L. Sun, Y. Liu and M. Zheng, *Small*, 2023, **20**, 2306323.
35 B. Wang, Y. Yu, H. Zhang, Y. Xuan, G. Chen, W. Ma, J. Li and J. Yu, *Angew. Chem., Int. Ed.*, 2019, **58**, 18443.
36 J. Ge and Y. Yin, *Angew. Chem., Int. Ed.*, 2011, **50**, 1492.
37 L. González-Urbina, K. Baert, B. Kolaric, J. Pérez-Moreno and K. Clays, *Chem. Rev.*, 2011, **112**, 2268.
38 R. Klajn, *Chem. Soc. Rev.*, 2014, **43**, 148–184.